Transport in Porous Media manuscript No.
(will be inserted by the editor)

Asymptotic analysis of unsteady ideal gas flow through layered porous media

Seth Keenan · Yana Nec

Abstract Temporal variability of boundary conditions is a common feature of certain fluid flows through a porous matrix, encountered, for instance, in landfill gas or natural gas collection, and sparging wells. Darcy's law subject to the weak compressibility of the fluid results in a non-linear partial differential equation for the pressure field. Slow variation admits asymptotic solutions for generic time dependence of the boundary forcing function, both as Dirichlet and Neumann conditions. Flow control strategies are suggested based on the asymptotic theory. A sealed outer domain boundary is identified as the configuration best amenable to full control of the pressure distribution via the induced well suction. Fast variation leads to a novel application of the classical compact support similarity solution in a domain with discontinuous parameters.

Keywords multiple layer porous media, time dependent non-linear problem, weakly compressible gas flow, flow control, asymptotic expansions

Mathematics Subject Classification (2010) 76S05, 35A35, 35C20, 35G20, 35G31, 35Q35

Article highlights

- † In most realistic cases the slow asymptotic regime governs the flow response to time dependent boundary conditions.
- † With a sealed outer boundary the spatio-temporal variation is decoupled, enabling full control of the pressure field.
- † Pressure time dependence obeys a similarity law throughout the domain with generic unsteady boundary conditions.

1 Background

Gas flow through a porous matrix of large dimensions is encountered in applications such as contaminated aquifer remediation, natural gas extraction and landfill gas collection. The purpose of a sparging well is to inject a fluid that will percolate through the matrix, binding to and neutralising detrimental compounds. By contrast, gas extraction wells induce suction to draw fluid out of the porous medium. In all three

S. Keenan
Department of Chemistry, Thompson Rivers University, Kamloops, British Columbia, Canada

Y. Nec
Department of Mathematics and Statistics, Thompson Rivers University, Kamloops, British Columbia, Canada
E-mail: ynec@tru.ca

systems the flow field is difficult to control in practice. Ideally the pressure distribution and flow rates in the system would depend monotonically on the pressure gradient exerted at the well. In reality the response to a variation of conditions at the well is often difficult to predict. In sparging wells this is evident via the erratic behaviour recorded by pressure probes (Lundegard and LaBrecque, 1995), in natural gas development basic flow models appear inadequate (Hyman et al., 2015), and in landfill gas collection the outlet suction is found to be an effective direct control mechanism in some settings (Kutsyi, 2015) and quite the opposite in others, cf. figure 3 of Nec and Huculak (2019).

Time dependent investigations in this area are scarce for two reasons. Mathematically the simplest description of a gas flow through a porous medium is via continuity of mass in conjunction with Darcy's law as the momentum transfer mechanism and the ideal gas equation of state accounting for weak compressibility effects. The governing equation ensuing is a non-linear partial differential equation in the fluid pressure p, but the steady version can be written as a linear ordinary differential equation in p^2. Consequently a predisposition toward analysing steady flow solutions developed. These were obtained for a one-dimensional framework (Wise and Townsend, 2011) and other simple geometries (Young, 1989), used in quasi-one-dimensional flow fields (Nec and Huculak, 2019; Feng et al., 2017), as well as constituted the end result of full numerical simulations in multiple spatial dimensions (Feng et al., 2015; Halvorsen et al., 2018; Keenan et al., 2021). From the vantage point of applications, the steady state is often the result of interest in the sparging process as well as natural or landfill gas collection. Furthermore, in the landfill application the porous matrix undergoes degradation, entailing significant permeability and gas generation rate changes. Consequently the service lifetime of quantitative models fit to site-specific measured data is brief, rendering their construction for the purpose of predicting future behaviour rarely worthwhile.

Therefore the prevailing approach towards the response to control parameters as well as sensitivity with respect to various physical conditions has revolved around scrutiny of steady state solutions at different regions of the relevant parameter space. Even when parameters are easily adjusted over the landfill's lifespan, each modelled state nonetheless corresponds to a steady flow (Keenan et al., 2021). The steady state modelling suffices to construe the impact of variability of intrinsic properties such as matrix permeability or fluid temperature, however there are situations when one is interested in the transient behaviour most often connected to changes induced or occurring on the boundary. Some examples, where this might be critical, are pump failure – full or partial – or water table fluctuation. If the system geometry is thought of as either a horizontal or vertical cylinder with a hollow core (the well), these correspond to changes in pressure and/or flux at the inner and outer boundaries of the domain respectively. Another example is possible changes in the atmospheric conditions for a horizontal landfill well that is temporarily uncovered or has a partly permeable cover. Whilst malfunctioning pumps are fixed within a given amount of time, eventuating in a return to steady conditions, water table and atmospheric pressure fluctuations are not controllable and might be seasonal or ongoing. Thus the changes in the boundary conditions might be fast or slow, periodically recurring or permanent. One essential aspect unifying them all is that the system operator would need a means to control the flow field in the face of the temporal variation to conform to certain regulations, for instance a maximal allowed pressure threshold or a minimal fraction of collected relative to generated mass in the landfill application (Conestoga-Rovers, 2010). To date there exists no theoretical basis for effective decision making in this regard.

In this study a new unsteady flow solution is derived for generic boundary conditions varying in time. Unsteady modelling is instrumental in providing insight into the response of the coupled well-matrix system and means of flow control in situations, where the transient is of more importance than the steady state, e.g. if regulation thresholds are exceeded, or where the transient is the reality over prolonged periods of time, i.e. no convergence to a steady state can be reasonably expected.

Landfill gas flow is used as the main example with the associated terminology adopted throughout, however all characteristics discussed as well as results and conclusions are equally applicable to any ideal gas flow through a porous medium of large spatial dimensions.

2 Governing equations

The continuity of mass for a fluid of density ρ flowing through a porous medium of porosity φ and generation rate C is given by (Fulks et al., 1971)

$$\frac{\partial}{\partial t}(\varphi\rho) + \nabla\cdot(\rho\mathbf{u}) = C, \tag{1a}$$

wherein $\mathbf{u}$ is the velocity vector. Pressure gradients in gas flow through the waste matrix, and natural gas or remediation fluid flow through the ground are small, rendering the assumption of ideal gas behaviour well tenable. Thus the relation between density ρ and pressure p is given by

$$p = \rho RT, \tag{1b}$$

where R and T are the gas constant and temperature respectively. By equation (1b) the density varies in proportion with the pressure. The quantitative range spanned by p is typically less than one tenth of its absolute value, implying that ρ varies little and designating this flow as weakly compressible. Furthermore, thermal equilibrium can be assumed (Young, 1989). The transfer of momentum is governed by Darcy's law (Whitaker, 1986)

$$\mathbf{u} = -\frac{\mathbf{K}}{\mu}\nabla p, \tag{1c}$$

where $\mathbf{K}$ is the permeability tensor and the fluid dynamic viscosity μ is computed for the gas mixture according to Davidson (1993). Albeit gravity is not readily negligible in these settings (Halvorsen et al., 2018), this study's salient focus is the response to time dependent boundary conditions and flow control strategies. The exclusion of gravity enables symmetric analytical solutions (Wise and Townsend, 2011; Young, 1989) as well as planar flow approximation within the cross-section of both horizontal and vertical wells as part of a semi-analytical model (Nec and Huculak, 2019; Feng et al., 2015, 2017). Horizontal landfill wells are typically hundreds of metres in length and collect gas at designated equidistant cross-sections, set a few tens of metres apart. The gas enters through either a cluster of apertures or a circumferential opening created by slightly overlapping telescopic pipes. Analysis of relative length scales shows that the longitudinal variation is small, justifying a planar description (Nec and Huculak, 2019). Vertical wells are a few tens of metres deep with continuously distributed perforations. Natural gas wells of either orientation similarly collect fluid along the entire length of the pipe with slow longitudinal variation. In a sparging well fluid is injected along the relevant length of the well within the aquifer. In all cases the intake area might be converted to an axisymmetric slit to obtain a planar approximation. All three applications involve anisotropic porous media of large physical dimensions with both directional and bulk variability of intrinsic properties. Without an extensive, site specific investigation the only practical approach is to divide the entire relevant matrix volume into sub-domains that, upon assigning a constant permeability, will give rise to a flow field having equivalent global characteristics, e.g. ranges of fluid pressure and velocity. Thus seeking axisymmetric planar flow solutions, combine (1c) and (1b) with (1a), express the differential operators in cylindrical coordinates and reduce $\mathbf{K}$ to an effective value k to read

$$\frac{\partial}{\partial t}(\varphi p) - \frac{1}{r}\frac{\partial}{\partial r}\left(\frac{k}{\mu} r p \frac{\partial p}{\partial r}\right) = RTC. \tag{2a}$$

To non-dimensionalise the problem, introduce the mappings $p \longmapsto p_n p'$, $r \longmapsto r_n r'$, $t \longmapsto t_n t'$, $k \longmapsto r_n^2 k'$, $\mu \longmapsto p_n t_n \mu'$ and $C \longmapsto C' p_n/(t_n RT)$, where the subscript n defines normalisation scales and the prime denotes respective non-dimensional quantities. Omitting the primes, equation (2a) becomes

$$\frac{\partial}{\partial t}(\varphi p) - \frac{1}{r}\frac{\partial}{\partial r}\left(\frac{k}{\mu} r p \frac{\partial p}{\partial r}\right) = C. \tag{2b}$$

Nec and Huculak (2019) proved the existence of a steady solution to (2b) in a domain comprising any number of contiguous rings with distinct permeability values. The methodology developed here is easily

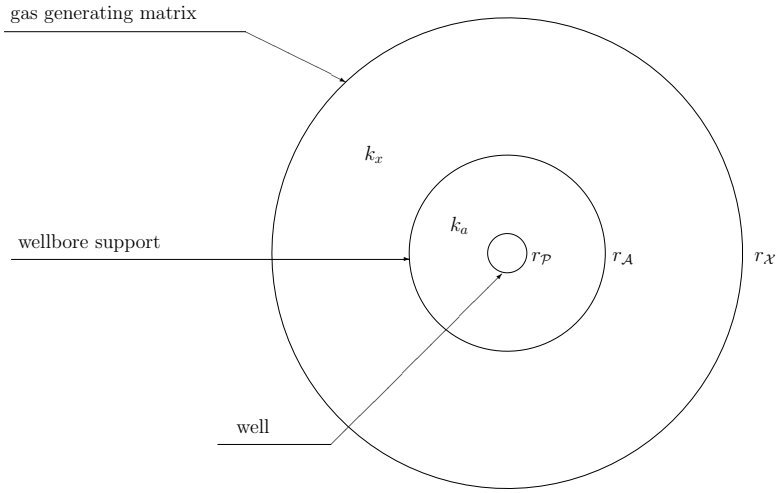

Fig. 1 Domain schematic and notation; dimensions not to scale

extended to that framework, but the exposition is highly technical and not instructive. To illustrate the construction of the unsteady asymptotic solution, the derivation hereunder is limited to two rings as in figure 1, with only the outer one generating gas. This corresponds to a common situation, where the bore is surrounded by a supporting lamina such as gravel or simply a depleted layer due to the well's proximity. The pipe radius is $r_{\mathcal{P}}$. The inner circle $\{r \mid 0 \leqslant r < r_{\mathcal{P}}\}$ must be excluded, as upon ingress into the pipe equation (2b) no longer holds, and the flow changes direction normal to the cross-section plane. The radius of the support lamina is $r_{\mathcal{A}}$. The outermost radius is $r_{\mathcal{X}}$. The respective permeabilities of the two annuli are k_a and k_x. Then the generation rate C, permeability k and porosity φ are given by

$$C = \begin{cases} 0 & r_{\mathcal{P}} < r < r_{\mathcal{A}} \\ C_b & r_{\mathcal{A}} < r < r_{\mathcal{X}} \end{cases}, \qquad k = \begin{cases} k_a & r_{\mathcal{P}} < r < r_{\mathcal{A}} \\ k_x & r_{\mathcal{A}} < r < r_{\mathcal{X}} \end{cases}, \qquad \varphi = \begin{cases} \varphi_a & r_{\mathcal{P}} < r < r_{\mathcal{A}} \\ \varphi_x & r_{\mathcal{A}} < r < r_{\mathcal{X}} \end{cases}. \tag{2c}$$

In the landfill application C is the mass of gas per unit volume and time generated within the medium. In a sparging well C vanishes throughout, as the fluid containing the remediation compounds of interest is injected at the boundary and propagates through the medium. In a natural gas well C should be set to zero where the fluid is only traversing the medium upon collection, or given a non-zero source term if the gas is known to be generated within the domain considered.

The boundary conditions accompanying (2b) are stated below for each solution setting. The initial condition is always the steady state solution conforming to $t = 0$ in the time dependent boundary conditions. On the contiguity circle $r = r_{\mathcal{A}}$ between domains of distinct matrix properties continuity of pressure and velocity (equivalently mass) is enforced:

$$p\left(r_{\mathcal{A}}^{-}, t\right) = p\left(r_{\mathcal{A}}^{+}, t\right). \tag{3a}$$

To obtain the condition for the velocity integrate (2b) with respect to r over an infinitesimally thin ring $(r_{\mathcal{A}} - \epsilon, r_{\mathcal{A}} + \epsilon)$ and take the limit $\epsilon \longrightarrow 0$. The discontinuities in φ and C entail no contribution, but the discontinuity in k yields

$$k_a \left.\frac{\partial p}{\partial r}\right|_{(r_{\mathcal{A}}^{-}, t)} = k_x \left.\frac{\partial p}{\partial r}\right|_{(r_{\mathcal{A}}^{+}, t)}, \tag{3b}$$

wherein condition (3a) was used.

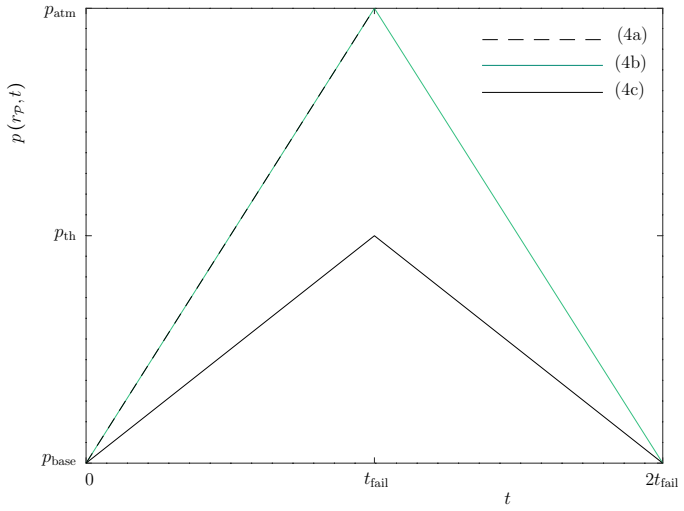

Fig. 2 Time dependent boundary condition $p(r_{\mathcal{P}}, t)$ as given by equations (4).

Suppose the well operates under a sub-atmospheric pressure p_{base} at steady state. Three time dependent scenarios were considered. At $t = 0$ the vacuum blower loses power over the time t_{fail} until the outlet is at atmospheric pressure:

$$p(r_{\mathcal{P}}, t) = p_{\mathrm{base}} + (p_{\mathrm{atm}} - p_{\mathrm{base}}) \frac{t}{t_{\mathrm{fail}}}, \qquad 0 \leqslant t \leqslant t_{\mathrm{fail}}. \tag{4a}$$

At t_{fail} an emergency blower engages and builds the vacuum back to its operational value:

$$p(r_{\mathcal{P}}, t) = \begin{cases} p_{\mathrm{base}} + (p_{\mathrm{atm}} - p_{\mathrm{base}}) \dfrac{t}{t_{\mathrm{fail}}} & 0 \leqslant t \leqslant t_{\mathrm{fail}} \\ \\ p_{\mathrm{atm}} + (p_{\mathrm{base}} - p_{\mathrm{atm}}) \dfrac{t - t_{\mathrm{fail}}}{t_{\mathrm{fail}}} & t_{\mathrm{fail}} \leqslant t \leqslant 2t_{\mathrm{fail}}. \end{cases} \tag{4b}$$

The emergency blower engages when the maximal pressure in the landfill exceeds a predetermined threshold at t_{fail} with the well pressure then equalling p_{th}:

$$p(r_{\mathcal{P}}, t) = \begin{cases} p_{\mathrm{base}} + (p_{\mathrm{th}} - p_{\mathrm{base}}) \dfrac{t}{t_{\mathrm{fail}}} & 0 \leqslant t \leqslant t_{\mathrm{fail}} \\ \\ p_{\mathrm{th}} + (p_{\mathrm{base}} - p_{\mathrm{th}}) \dfrac{t - t_{\mathrm{fail}}}{t_{\mathrm{fail}}} & t_{\mathrm{fail}} \leqslant t \leqslant 2t_{\mathrm{fail}}. \end{cases} \tag{4c}$$

The conceptual difference of (4c) is that t_{fail} is not known in advance. The respective plots are given in figure 2. As part of the asymptotic theory developed below, a linearisation of the governing equation (2b) was performed. For some combinations of asymptotic parameters and boundary conditions it was important to understand whether an ensuing linear pressure distribution was the result of the linearised equation or linear forcing. To that end a non-linear smooth variation $\sin\big(\pi t \big/ (2t_{\mathrm{fail}})\big)$ with an appropriate amplitude replacing the linear ramp was tested.

In order to verify the asymptotic theory the FlexPDE solver (PDE Solutions Inc., 2016) was used to obtain a finite element solution of (2b) subject to (4) on an unstructured triangular, dynamically refined mesh with a prescribed relative error in p (non-dimensionalised by p_{atm}) of 10^{-6}. Table 1 lists the nominal set of parameters used in computations throughout unless noted specifically in pertinent figure captions. Negative pressure values are relative to the atmosphere.

parameter	symbol	value
pipe radius	$r_{\mathcal{P}}$	0.0762 m (3 in)
temperature	T	15°C
steady state suction pressure	p_{base}	−3.75 kPa
steady state surface pressure	$p_{\mathcal{X}}$	1 atm
layer b generation rate	C_b	0.004 kg/(m^{3}hr)
CH_4 molar fraction		0.5
O_2 molar fraction		0.01
CO_2 molar fraction		0.4
layer a thickness	$r_{\mathcal{A}} - r_{\mathcal{P}}$	1 m
layer b thickness	$r_{\mathcal{X}} - r_{\mathcal{A}}$	8 m
layer a porosity	φ_a	0.35
layer b porosity	φ_x	0.2

Table 1 Parameters of a single landfill cell common to all examples solved numerically

3 Slow variation regime

A quasi-steady variation occurs when $t_{\text{fail}} \gg 1$. Define a small asymptotic parameter $\epsilon = 1/t_{\text{fail}} \ll 1$ and a slow time scale $\tau = \epsilon t$. Then any stage in (4) can be generalised as $p(r_{\mathcal{P}}, \tau) = p_{\text{init}} + m_{\text{fail}}\tau$, where both the pressure p_{init} and slope m_{fail} are ϵ-independent. More generally this boundary condition might be set as

$$p(r_{\mathcal{P}}, \tau) = p_{\text{well}}(\tau), \tag{5a}$$

such that $p_{\text{well}}(\tau) \sim \mathcal{O}(1)$ and ϵ-independent. For this initial example of the asymptotic construction a zero normal flux condition is taken on the outermost domain boundary. In practice this pertains to three situations. One possibility is that the modelled flow field indeed has an impervious boundary, such as an impermeable membrane lining a landfill, or a natural gas well surrounded by a wall of solid rock or clay. The second option is that there is no physical boundary, but one is interested in the well's zone of influence, i.e. the domain extending from the well to the point, where it can no longer collect fluid. At that point the fluid's radial velocity reverses and normal flux equals zero. Landfill wells are often installed in a lattice-like formation inducing a tessellation of zones of influence. On the boundaries of neighbouring zones the normal flux must vanish. In both square and hexagonal arrangements the zones can be approximated by an inscribed circle. In reality the lattice is likely to be somewhat irregular. Nonetheless each well draws fluid radially, and therefore the zone's main shape can be represented by a circle. At its tangency points with the true contour the flux will indeed vanish. On the arcs in between it will be small. It is to be shown below that the condition of vanishing radial flux effectively decouples the temporal and radial variation, endowing the operator with a useful control strategy.

A no flux condition on the outermost boundary implies

$$\left.\frac{\partial p}{\partial r}\right|_{(r_{\mathcal{X}}, \tau)} = 0. \tag{5b}$$

Introduce the asymptotic series

$$p = p_0(r, \tau) + \epsilon\, p_1(r, \tau) + \epsilon^2 p_2(r, \tau) + \cdots. \tag{6}$$

Substituting (6) into (2b), applying the chain rule whereby $\partial_t = \epsilon\partial_\tau$, and collecting terms of equal orders, yields at $\mathcal{O}(1)$

$$\frac{1}{r}\frac{\partial}{\partial r}\left(r p_0 \frac{\partial p_0}{\partial r}\right) = -\frac{\mu C}{k}, \tag{7a}$$

and at $\mathcal{O}(\epsilon)$

$$\frac{1}{r}\frac{\partial}{\partial r}\left(r\frac{\partial}{\partial r}(p_0 p_1)\right) = \frac{\mu\varphi}{k}\frac{\partial p_0}{\partial \tau}. \tag{7b}$$

The general solution of (7a) is

$$p_0^2 = -\frac{\mu C}{2k}r^2 + A_0(\tau)\ln r + B_0(\tau), \tag{8a}$$

where the functions $A_0(\tau)$ and $B_0(\tau)$ are to be determined from boundary conditions (5) and continuity conditions (3). When these are constant, (8a) is the steady state solution (Nec and Huculak, 2019). For $\tau = 0$ it is also the initial condition for (2b). The general solution to (7b) is given by

$$p_0 p_1 = \frac{\mu\varphi}{2k}\int\frac{1}{r}\int^r \frac{\tilde{r}}{p_0(\tilde{r},\tau)}\Big(A_0'\ln\tilde{r} + B_0'\Big)\mathrm{d}\tilde{r}\,\mathrm{d}r + A_1(\tau)\ln r + B_1(\tau), \tag{8b}$$

where both integrals are indefinite, and $A_1(\tau)$ and $B_1(\tau)$ need to be similarly determined from (5) and (3). The boundary conditions on p must be expressed in terms of the slow time scale τ, so as to provide boundary conditions for all terms p_i in the asymptotic expansion (6). Therefore

$$p_0\left(r_{\mathcal{P}},\tau\right) = p_{\mathrm{well}}(\tau), \qquad p_i\left(r_{\mathcal{P}},\tau\right) = 0 \quad \forall\ i \geqslant 1, \tag{9a}$$

$$\left.\frac{\partial p_i}{\partial r}\right|_{(r_{\mathcal{X}},\tau)} = 0 \quad \forall\ i \geqslant 0. \tag{9b}$$

The continuity equations (3) must hold at every order, i.e. for all p_i, and for more elegant implementation might be written at orders $\mathcal{O}(1)$ and $\mathcal{O}(\epsilon)$ respectively as

$$p_0^2\left(r_{\mathcal{A}}^-,\tau\right) = p_0^2\left(r_{\mathcal{A}}^+,\tau\right), \qquad k_a\left.\frac{\partial p_0^2}{\partial r}\right|_{(r_{\mathcal{A}}^-,\tau)} = k_x\left.\frac{\partial p_0^2}{\partial r}\right|_{(r_{\mathcal{A}}^+,\tau)}, \tag{10a}$$

and

$$\left.(p_0 p_1)\right|_{(r_{\mathcal{A}}^-,\tau)} = \left.(p_0 p_1)\right|_{(r_{\mathcal{A}}^+,\tau)}, \qquad k_a\left.\frac{\partial}{\partial r}(p_0 p_1)\right|_{(r_{\mathcal{A}}^-,\tau)} = k_x\left.\frac{\partial}{\partial r}(p_0 p_1)\right|_{(r_{\mathcal{A}}^+,\tau)}. \tag{10b}$$

Writing (8a) separately for each layer with superscripts $(\,\cdot\,)^{(a)}$ and $(\,\cdot\,)^{(b)}$ referring to the first (non-generating) and second (potentially generating) annuli

$$p_0^{(a)\,2} = A_0^{(a)}(\tau)\ln r + B_0^{(a)}(\tau), \tag{11a}$$

$$p_0^{(b)\,2} = -\frac{\mu C_b}{2k_x}r^2 + A_0^{(b)}(\tau)\ln r + B_0^{(b)}(\tau), \tag{11b}$$

and enforcing (9) and (10a) yields

$$A_0^{(b)} = \frac{\mu C_b}{k_x}r_{\mathcal{X}}^2, \tag{12a}$$

$$A_0^{(a)} = \frac{k_x}{k_a}\left(A_0^{(b)} - \frac{\mu C_b}{k_x}r_{\mathcal{A}}^2\right), \tag{12b}$$

$$B_0^{(a)} = p_{\mathrm{well}}^2(\tau) - A_0^{(a)}\ln r_{\mathcal{P}}, \tag{12c}$$

$$B_0^{(b)} = \left(A_0^{(a)} - A_0^{(b)}\right)\ln r_{\mathcal{A}} + B_0^{(a)} + \frac{\mu C_b}{2k_x}r_{\mathcal{A}}^2. \tag{12d}$$

From (12a) and (12b) $A_0'(\tau)$ in (8b) vanishes. By (12c) and (12d) $B_0' = 2p_{\mathrm{well}}(\tau)p_{\mathrm{well}}'(\tau)$ in both layers. It is now possible to choose convenient bounds for the indefinite integrals in (8b):

$$\left(p_0 p_1\right)^{(a)} = \frac{\mu\varphi_a}{2k_a}B_0'\int_{r_{\mathcal{P}}}^{r}\frac{1}{\tilde{r}}\int_{r_{\mathcal{A}}}^{\tilde{r}}\frac{\varrho\,\mathrm{d}\varrho}{p_0^{(a)}(\varrho,\tau)}\,\mathrm{d}\tilde{r} + A_1^{(a)}(\tau)\ln r + B_1^{(a)}(\tau), \tag{13a}$$

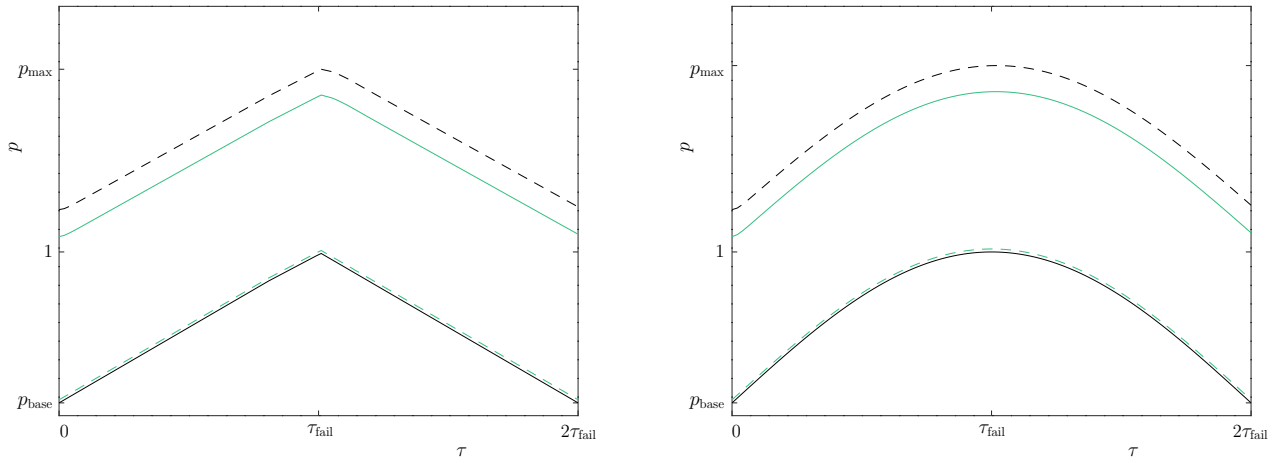

Fig. 3 Example of direct dependence of the pressure field $p(r,\tau)$ on the well boundary function $p_{\text{well}}(\tau)$ (solid black) under a slow variation regime with a sealed outer boundary: $r = r_{\mathcal{A}}$ (dashed green/grey, edge of layer a), $r = \left(r_{\mathcal{A}} + r_{\mathcal{X}}\right)/2$ (solid green/grey, centre of layer b) and $r = r_{\mathcal{X}}$ (dashed black, edge of layer b) for linear (left) and sinusoidal (right) forcing. $\epsilon = 0.1$, $k_a = 1\text{e}-06\text{m}^2$, $k_x = 1\text{e}-08\text{m}^2$, all other parameters listed in table 1.

$$\left(p_0 p_1\right)^{(b)} = \frac{\mu\varphi_x}{2k_x} B_0' \int_{r_{\mathcal{A}}}^{r} \frac{1}{\tilde{r}} \int_{r_{\mathcal{X}}}^{\tilde{r}} \frac{\varrho \,\mathrm{d}\varrho}{p_0^{(b)}(\varrho,\tau)} \,\mathrm{d}\tilde{r} + A_1^{(b)}(\tau) \ln r + B_1^{(b)}(\tau). \tag{13b}$$

Enforcing (9) and (10b) yields

$$A_1^{(b)} = 0, \tag{14a}$$

$$A_1^{(a)} = \frac{\mu\varphi_x}{2k_a} B_0' \int_{r_{\mathcal{X}}}^{r_{\mathcal{A}}} \frac{\varrho \,\mathrm{d}\varrho}{p_0^{(b)}(\varrho,\tau)}, \tag{14b}$$

$$B_1^{(a)} = -A_1^{(a)} \ln r_{\mathcal{P}}, \tag{14c}$$

$$B_1^{(b)} = \frac{\mu\varphi_a}{2k_a} B_0' \int_{r_{\mathcal{P}}}^{r_{\mathcal{A}}} \frac{1}{\tilde{r}} \int_{r_{\mathcal{A}}}^{\tilde{r}} \frac{\varrho \,\mathrm{d}\varrho}{p_0^{(a)}(\varrho,\tau)} \,\mathrm{d}\tilde{r} + A_1^{(a)} \ln \frac{r_{\mathcal{A}}}{r_{\mathcal{P}}}. \tag{14d}$$

With (11)–(14) the combined solution (6) can be written as

$$p(r,\tau) \sim p_{\text{well}}(\tau) \sqrt{1 + \frac{f_0(r)}{p_{\text{well}}^2(\tau)}} + \epsilon\, p_{\text{well}}'(\tau) f_1(r,\tau) \Big/ \sqrt{1 + \frac{f_0(r)}{p_{\text{well}}^2(\tau)}} + \mathcal{O}\left(\epsilon^2\right), \tag{15}$$

demonstrating that to leading order the boundary forcing function $p_{\text{well}}(\tau)$ unequivocally dictates the temporal evolution throughout the domain: at any chosen value of r the pressure $p^2(r,\tau)$ will be a mere shift of $p_{\text{well}}^2(\tau)$. Figure 3 exemplifies this result for both a linear ramp and sinusoidal well pressure variation. This behaviour is solely a consequence of the no flux condition (9b) that renders a cascade of potentially τ-dependent functions constant. When (15) holds, the well operator has full control over the pressure distribution in the system via the suction imposed.

More complicated circumstances, for instance, a Neumann condition with a non-zero flux or a Dirichlet condition on p, constant or otherwise, begets a non-trivial coupling that results in a replacement of the function $f_0(r)$ in (15) by a function of both r and τ similar to $f_1(r,\tau)$. Both problems are solved in appendix A with generic time dependent boundary conditions $p(r_{\mathcal{P}},\tau) = p_{\text{well}}(\tau)$ and $p(r_{\mathcal{X}},\tau) = p_{\mathcal{X}}(\tau)$. The latter is useful, for instance, when the barometric pressure fluctuates.

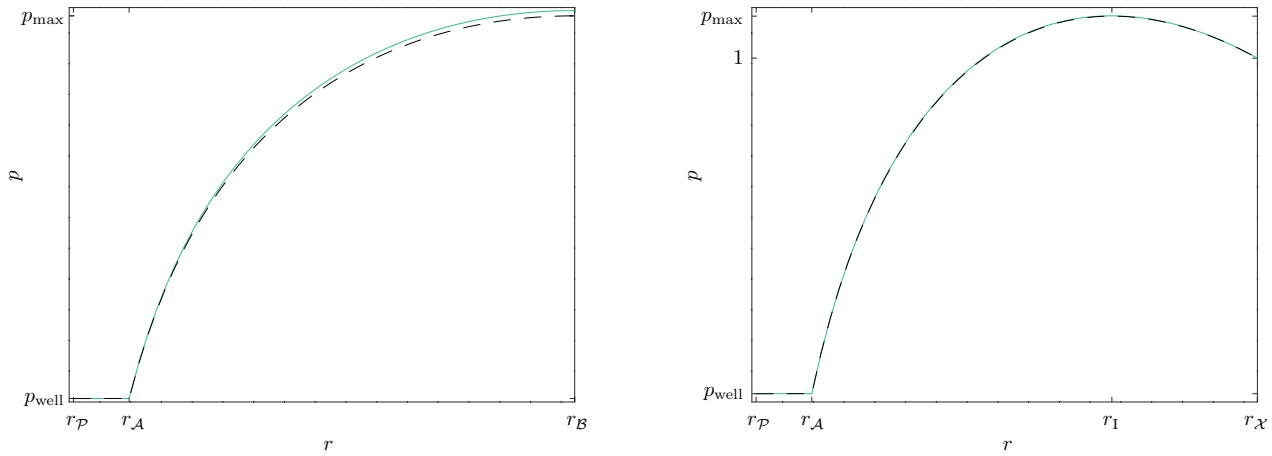

Fig. 4 Example of similarity effect in the pressure profile $p(r,\tau)$ under a slow variation regime with linear forcing $p_{\text{well}}(\tau)$ for flux (left) and pressure (right) condition on the outer boundary for $\tau = 0.75$: $\epsilon = 0.1$, $t = 7.5$ (green/grey); $\epsilon = 0.005$, $t = 150$ (dashed black). $k_a = 1\text{e}-04\text{m}^2$, $k_x = 1\text{e}-08\text{m}^2$, all other parameters listed in table 1.

3.1 Similarity with respect to τ

At times in asymptotic analysis the small parameter ϵ might have a physical meaning without the necessity to specify an explicit value for it. A prominent example is the derivation of weakly non-linear amplitude equations near a bifurcation point of a dynamical system, such as the Ginzburg-Landau equation. The proximity to the bifurcation point is cast into a small asymptotic scale, but the exact measure whereby the bifurcation point is exceeded, is immaterial. By contrast, in this problem ϵ corresponds to a parameter, whose value has an immediate bearing on the solution. The definitions of the asymptotically small parameter $\epsilon = 1/t_{\text{fail}}$ and slow time scale $\tau = \epsilon t$ imply that if both ϵ and t were to be mapped $\epsilon \longmapsto \epsilon/\alpha$ and $t \longmapsto \alpha t$ for any positive constant $\alpha \sim \mathcal{O}(1)$, τ would remain the same. Therefore at the limit $\epsilon \longrightarrow 0^+$ the solutions $p(r,\tau)$ corresponding to the choices $\{\epsilon, t\}$ and $\{\epsilon/\alpha, \alpha t\}$ must be identical for arbitrary functions $p_{\text{well}}(\tau)$ and $p_{\mathcal{X}}(\tau)$. Such an ability to unify distinct solutions via an invariant compound containing one or more independent variables is known as similarity or affinity.[1] When ϵ is small, but finite, the quantitative accuracy of this identity is an indication of the robustness of the asymptotic solution akin to the rapidity of convergence of the asymptotic expansion. Figure 4 illustrates this phenomenon for basic boundary conditions and a premeditated extreme choice of parameters: a difference of four orders of magnitude in layer permeability and at least one in t and ϵ. Observe that when pressure is prescribed on the outer circle (Dirichlet condition), the curves are indistinguishable, whilst for a prescribed velocity (vanishing or not, Neumann condition) a minor discrepancy is evident. Lesser disparity in any of the foregoing parameters improves the agreement. Non-linear forcing yielded a match of a comparable quality and is not shown.

The soundness of the similarity effect with arbitrary $p_{\mathcal{X}}(\tau)$ was confirmed in a simulation of a possible fluctuation of the barometric pressure in conjunction with (4b). For instance, if during a passing weather front the pressure drops from $p_{\text{atm}} + \Delta p_{\text{bar}}$ to $p_{\text{atm}} - \Delta p_{\text{bar}}$ over a period of time equal to $t_{\text{fail}}/2$, $p_{\mathcal{X}}(\tau)$

[1] In geometry and especially fractal geometry different definitions of dimensional measures for the geometric object in question led to a conceptual distinction between the two (Mandelbrot, 1985; Lakhtakia et al., 1986), however in the context of dynamical systems similarity is only one instance in a whole family of affine transformations. In this study two separate similarity mechanisms arise: one involves the slow time scale τ and pertains to the robustness of the asymptotic solution; the other appears as part of the reduction of the partial differential equation to an ordinary one in §4 and will be referred to as an affinity transformation to avoid confusion.

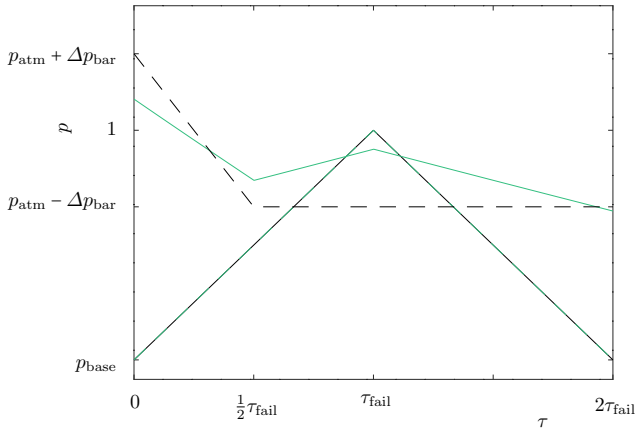

Fig. 5 Pressure history $p(r,\tau)$ under a slow variation regime with asynchronous linear variation on both boundaries: $p_{\text{well}}(\tau)$ (solid black), $r = r_{\mathcal{A}}$ (dashed green/grey, edge of layer a, visually indistinguishable from $p_{\text{well}}(\tau)$), $r = \big(r_{\mathcal{A}} + r_{\mathcal{X}}\big)/2$ (solid green/grey, centre of layer b) and $r = r_{\mathcal{X}}$ (dashed black, edge of layer b). $\epsilon = 0.05$, $k_a = 1\text{e}-04\text{m}^2$, $k_x = 1\text{e}-08\text{m}^2$, all other parameters listed in table 1.

might be expressed as

$$p_{\mathcal{X}}(\tau) = \begin{cases} p_{\text{atm}} + \Delta p_{\text{bar}} - 4\Delta p_{\text{bar}}\,\dfrac{t}{t_{\text{fail}}} & 0 \leqslant t \leqslant t_{\text{fail}}/2 \\ \\ p_{\text{atm}} - \Delta p_{\text{bar}} & t \geqslant t_{\text{fail}}/2. \end{cases} \tag{16}$$

Figure 5 depicts the resulting temporal dependence of pressure at the points of import in the domain: due to the asynchronous variation imposed on the boundaries the progression of profiles from the well outwards is no longer monotonic, cf. figure 3. Nevertheless the quality of agreement of the pressure profiles throughout the domain for a fixed τ comprising distinct pairs of t and ϵ, is as outstanding as shown in the right panel of figure 4 for constant $p_{\mathcal{X}}$. The agreement is equally good for a sinusoidal non-linearity $\sin\big(\pi t\big/(4t_{\text{fail}})\big)$ with an appropriate amplitude. The connection with the convergence of the asymptotic series is explored below.

3.2 Asymptotic solution: error analysis

The quality of the foregoing asymptotic solution is underpinned by two unrelated elements. One is directly related to the asymptotic construction: for series (6) to hold and converge sufficiently quickly, the application must indeed comply with the assumption of a slowly varying boundary condition. Whilst (4) easily conforms to this requirement throughout most of the specified time intervals, very close to the initial point $t = 0$ and the reversal point $t = t_{\text{fail}}$ in (4b) and (4c), the following problem arises. Before $t = \tau = 0$ the system is at a steady state, i.e. $\partial_t p \equiv \partial_\tau p \equiv 0$. Immediately after $t = 0$ the linear slope $\partial_\tau p$ is finite for any value of $\epsilon > 0$ (including at the limit $\epsilon \longrightarrow 0^+$). As a result $\partial_\tau p$ has the form of the Heaviside step function. In (4b) and (4c) the same abrupt change of slope occurs when the emergency blower engages. In a numerical solution this discontinuity would require a non-uniform adjustment of the time step to maintain a prescribed accuracy. In the asymptotic solution the non-uniformity appears in the error, since ϵ is fixed.

The second element impacting the asymptotic solution's ability to capture the true solution correctly is the permeability disparity between the two porous laminae. Gravel to waste permeability ratio is known to span one to four orders of magnitude. Similar disparity characterises pervious to semi-impervious ground types. The higher the ratio, the steeper the pressure gradient and slope jump at the contiguity circle, as is gleaned from (12b) and (3b).

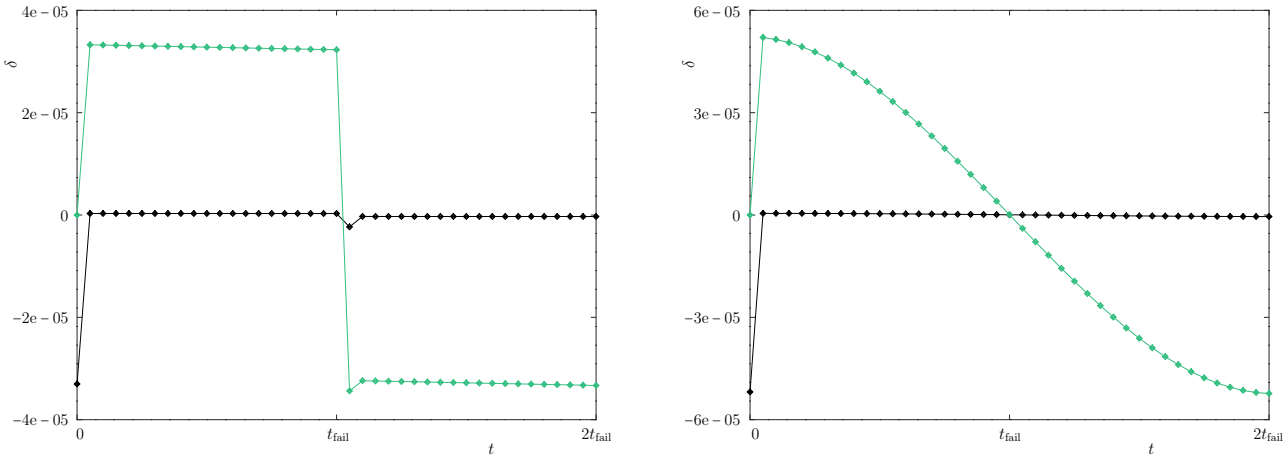

Fig. 6 Asymptotic solution maximal error as defined by (6) under a slow variation regime with a sealed outer boundary: $\delta_1 = p - p_0 \sim \mathcal{O}(\epsilon)$ and $\delta_2 = p - p_0 - \epsilon p_1 \sim \mathcal{O}\left(\epsilon^2\right)$ (green/grey and black respectively) with linear (left) and sinusoidal (right) forcing. $\epsilon = 0.005$, $k_a = 1\text{e}-04\text{m}^2$, $k_x = 1\text{e}-08\text{m}^2$, all other parameters listed in table 1.

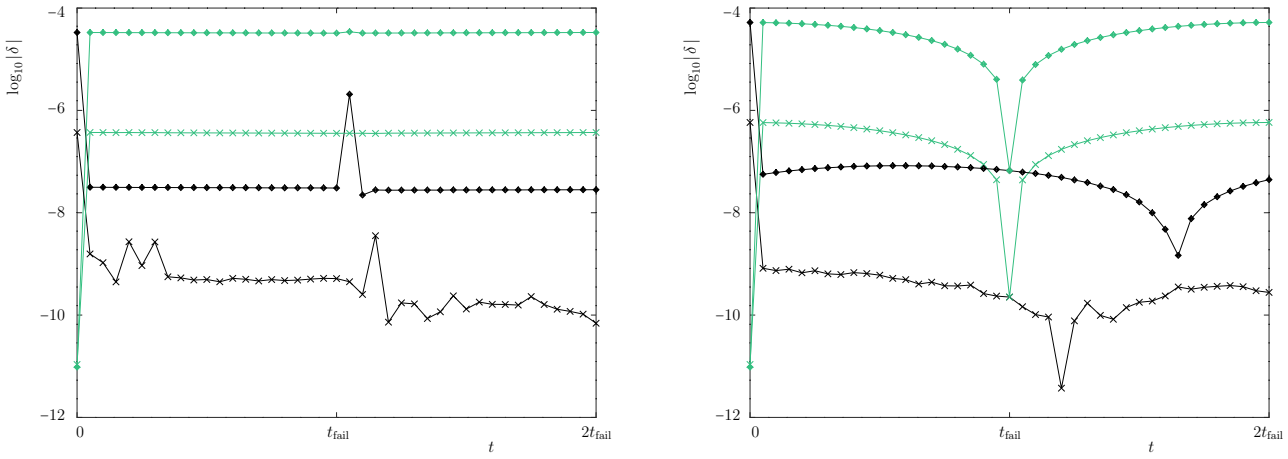

Fig. 7 Asymptotic solution maximal log error as defined by (6) under a slow variation regime with a sealed outer boundary: $\delta_1 = p - p_0 \sim \mathcal{O}(\epsilon)$ and $\delta_2 = p - p_0 - \epsilon p_1 \sim \mathcal{O}\left(\epsilon^2\right)$ (green/grey and black respectively) with linear (left) and sinusoidal (right) forcing. $\epsilon = 0.005$, $k_a = 1\text{e}-04\text{m}^2$, $k_x = 1\text{e}-08\text{m}^2$ (diamonds) and $k_x = 1\text{e}-06\text{m}^2$ (crosses), all other parameters listed in table 1.

The two effects are closely interwoven. With a sufficiently small ϵ and moderate permeability ratio, the error that the abrupt change in the derivative $\partial_\tau p$ is responsible for decays quickly in time. With an impervious outer boundary and the time variation imposed on the well boundary, the maximal error is obtained at the outer circumference of the domain. Figure 6 depicts a typical maximal error with $\epsilon = 0.005$ and $k_a/k_x = 10^4$ for linear and sinusoidal $p_{\text{well}}(\tau)$. Whilst both have a Heaviside step-like shape near $t = 0$, with the latter both the first and second order errors are smooth at t_{fail}. Consistent with the phenomenon of similarity discussed above, the error diminishes whenever similarity improves, and under favourable conditions (such as moderate permeability disparity) reduces to the numerical solution scheme error.

The error magnitude increases with ϵ: up to $\epsilon = 0.1$ it grows proportionately in absolute value, uniformly in time, and maintains the qualitative behaviour shown in figure 6, however for $\epsilon > 0.1$ the convergence of (6) might require additional terms for proper error control. The error diminishes when the disparity

in k_a/k_x is reduced, approximately one order of magnitude per one order of magnitude of the ratio. An example is shown in figure 7 on a logarithmic scale. For extreme (and rarely encountered in real landfills) ratios $k_a/k_x > 10^4$ the error deteriorates without the use of higher order terms. In most practical situations with $t_{\text{fail}} \geqslant 1\text{sec}$ two terms of the asymptotic expansion will give a maximal error on the order of $\mathcal{O}\left(10^{-5}\right)$ or better, i.e. the dimensional pressure variable will be determined to the accuracy of 1Pa or less, never exceeding the tolerance attained by digital instrumentation of professional grade.

4 Fast variation regime

When the temporal variation of the induced outlet vacuum is abrupt, the response throughout the domain becomes strongly non-linear and can no longer be captured via an asymptotic solution. Realistic scenarios might include a power failure (4a) as well as power spikes (4b) and (4c). Mathematically the parameter t_{fail} in (4) is taken very small, i.e. $t_{\text{fail}} = \epsilon \ll 1$. The corresponding fast time scale is $\tau = t/\epsilon$, rendering the integration of equation (2b) formally stiff.

The left-hand side of equation (2b) is the polar version of the classical non-linear diffusion operator $\partial_t - \Delta(\,\cdot\,)^\gamma$ that is fundamental in porous media flow (Barenblatt et al., 1990). Within each landfill layer appropriate scaling of the independent variables t and r in (2b) results in a parameter free form

$$\frac{\partial p}{\partial \tau} - \frac{1}{\varrho}\frac{\partial}{\partial \varrho}\left(\varrho p \frac{\partial p}{\partial \varrho}\right) = 0, \qquad \tau = \frac{t}{\varphi}, \quad \varrho = \frac{r}{\sqrt{\mu/k}}, \quad C = 0 \tag{17a}$$

or

$$\frac{\partial p}{\partial \tau} - \frac{1}{\varrho}\frac{\partial}{\partial \varrho}\left(\varrho p \frac{\partial p}{\partial \varrho}\right) = 1, \qquad \tau = \frac{t}{\varphi C}, \quad \varrho = \frac{r}{\sqrt{\mu C/k}}, \quad C \neq 0. \tag{17b}$$

The homogeneous part of (17) is the one-dimensional polar form of what is known as the porous medium equation or non-linear diffusion equation employed in numerous dispersion problems in a variety of applications involving fluids other than a weakly compressible ideal gas and going as far back as the early 1960s (King, 1988, and references therein). The Cartesian form of (17a) has seen extensive theoretical work in the context of renormalisation group and affinity transformation specifically for porous media flow (Barenblatt, 1996). Simplistic dimensional analysis implies the existence of an affinity solution $p(\xi)$ with $\xi = r^2/t$. The classical framework interweaves two assumptions: the sought solution is a function of compact support, and the boundary conditions are chosen so as to allow the usage of the affinity variable ξ (Volpert et al., 2018). Equation (17a) has a number of easily constructed exact solutions:

$$p_{\text{ex}}(\varrho, \tau) = \frac{\varrho^2}{8(\tau_o - \tau)}, \qquad p_{\text{ex}}(\varrho, \tau) = \left(\frac{\tau_o}{\tau}\right)^{1/2} - \frac{\varrho^2}{8\tau}. \tag{18}$$

Both are reminiscent of an affinity solution (the former is equivalent to one due to the translational invariance in τ, whereas the latter does not qualify), and neither satisfies the required boundary conditions, the degree of freedom τ_o notwithstanding. The Cartesian version $\partial_\tau p - \frac{1}{2}\partial_\varrho^2 p^2 = 0$ possesses closely related solutions with slightly adjusted constants and additional two wave-like solutions $p_{\text{ex}}(\varrho, \tau) = \tau \pm \varrho$. Equation (17b) does not admit affinity solutions of this kind due to the inhomogeneous right-hand side or possess any exact solutions to the authors' knowledge. The purpose of this section is to outline when the reduction to an ordinary differential equation via an affinity variable might be attained in the current problem, and discuss the reasons that the corresponding parametric space is limited.

Lamina a is narrow relative to the main matrix layer b and is in place to support the well. Therefore even when the boundary condition on the well varies abruptly (yet continuously), the pressure within lamina a responds in the same way as in the slow regime. In other words, to disrupt the asymptotic solution in lamina a alone the temporal variation must for all intents and purposes be a step discontinuity. By contrast, the response within layer b is characterised by significant reaction time that increases with the permeability ratio k_a/k_x. Figure 8 illustrates the expected delay in pressure adjustment at $r = (r_{\mathcal{A}} + r_{\mathcal{X}})/2$ (centre of layer b) for $k_a/k_x = 10^4$.

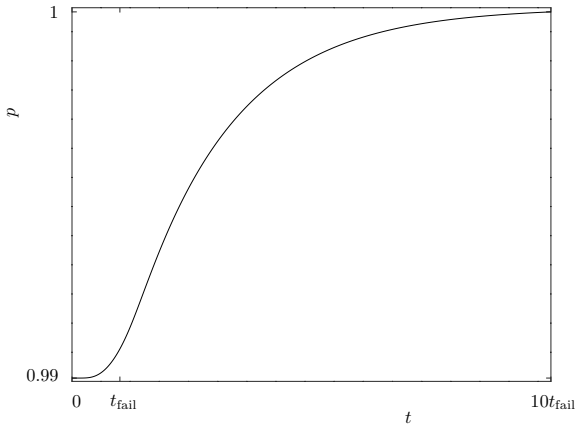

Fig. 8 Pressure history $p\big((r_{\mathcal{A}}+r_{\mathcal{X}})/2,t\big)$ under a fast variation regime with linear forcing. $t_{\text{fail}}=0.01\text{sec}$, $k_a=1\text{e}-04\text{m}^2$, $k_x=1\text{e}-08\text{m}^2$, all other parameters listed in table 1.

In the current problem (17a) holds within lamina a. Albeit formally (17b) is qualitatively distinct from (17a), the contribution of the inhomogeneity to the pressure profile induced by a properly functioning well is small (Nec and Huculak, 2019). Realistic situations, where this is not so, are usually a result of incorrect design in conjunction with little control over the content or structure of the porous medium, and can be classified as follows in the order of ascending rarity: impervious outer boundary; strong outward (positive) flux on the outer boundary; layer b permeability significantly exceeding that of layer a (several orders of magnitude). Therefore one might expect that the inherent affinity variable of (17a) would be useful upon setting $C=0$ throughout as an approximation to a realistic landfill with a partly permeable boundary and moderate negative flux thereon. In sparging wells the generation rate is by definition zero. In natural gas extraction the approximation is relevant where no significant active generation takes place, i.e. the well only induces fluid flow similarly to the sparging well, but in the reverse direction. Such a reduction of the partial differential equation (2b) could be potentially valuable, as the resulting ordinary differential equation must be solved only once, therefore its solution could be stored and evaluated as needed at any desired r and t values. In other words, neglecting the contribution of a non-zero generation rate for the sake of a pre-computed solution readily available to designers and field operators unequipped to solve partial differential equations might be well justified.

The qualitative disparity between (2b) and the ostensibly similar dispersion problems of the type solved in Volpert et al. (2018) is trifold. One, herein the domain is fixed and $r>0$, whereas conventionally the fluid concentration is non-zero over an ever growing domain encompassing the origin, albeit the support of the radial profile function remains compact at all times. Two, in the well problem the physical interpretation of the sought pressure distribution function p is such that it can never approach zero. And three, (2b) comes with a discontinuity in the permeability parameter k and porosity φ that must remain even if one is willing to neglect the generation rate in layer b, thereby eliminating the discontinuity in C. From a technical vantage point, it is necessary to solve (17a) in two adjacent domains and match the solutions so as to create a C^0 function over the combined domain subject to the continuity conditions (3). This can only be accomplished with an iterative procedure as detailed below.

Observe that the classical affinity variable $\xi=r^2/t$ might fail to support a boundary condition with $r>0$ at $t=0$. Thus the derivation hereinafter was done for $\zeta=\big(r^2/t\big)^{\beta}$, where the arbitrary power β might be negative. Of course, the final solution must be identical for all viable values of β, and this feature was used to confirm the correctness of the implemented algorithm. Moreover, in certain instances using $\beta\neq 1$ aided with the implicit integration stiffness described in §3.2. As long as ϵ is not taken extremely small and the instant of the discontinuity in $\partial_\tau p$ is avoided, the stiffness is manageable, permitting the use of the built-in Octave function `ode45` with an absolute tolerance of 10^{-6} and an adaptive time step (GNU Octave, 2021). Setting $C=0$ in (2b) and converting to an ordinary differential equation in ζ in any of the domain

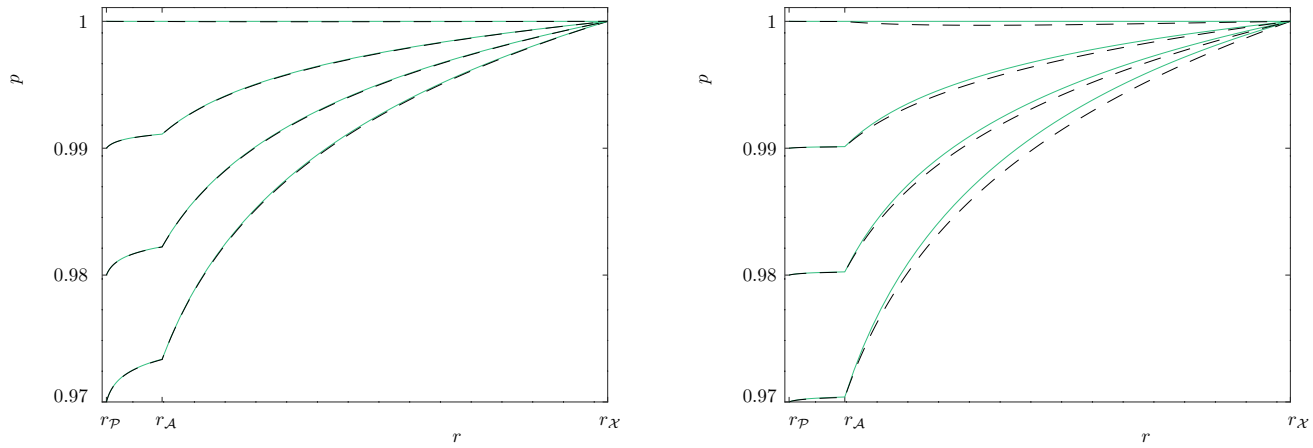

Fig. 9 Comparison of affinity solution $p(\zeta)$ (green/grey) and full solution $p(r,\tau)$ (dashed black) under a fast variation regime with linear forcing $p_{\text{well}}(\tau)$ for low (left, $k_a/k_x = 10$) and moderate (right, $k_a/k_x = 100$) lamina permeability ratio. $t_{\text{fail}} = 0.01$sec. The curves correspond to $t/t_{\text{fail}} = \left\{\frac{1}{4}, \frac{1}{2}, \frac{3}{4}, 1\right\}$ monotonically bottom to top. $k_a = 1\text{e}-04\text{m}^2$, all other parameters listed in table 1.

annuli with fixed values of k and φ yields

$$\alpha p' + \frac{\beta}{\zeta^{1/\beta}}\left(\zeta p p'\right)' = 0, \qquad \alpha = \frac{\varphi\mu}{4k}, \tag{19}$$

wherein primes denote differentiation with respect to ζ. The exact solution $p_{\text{ex}}(\zeta) = -\frac{\alpha}{2}\zeta^{1/\beta}$ is not physical (since p cannot be negative) and due to the non-linearity of (19) is not helpful in the reduction of order. Defining $y_1 = p$ and $y_2 = \zeta p'$,

$$\begin{pmatrix} y_1 \\ y_2 \end{pmatrix}' = \begin{pmatrix} y_2/\zeta \\ -\dfrac{1}{y_1}\left(\dfrac{\alpha}{\beta} y_2 \zeta^{1/\beta-1} + \dfrac{y_2^2}{\zeta}\right) \end{pmatrix}. \tag{20a}$$

This first order non-linear ordinary differential system was solved iteratively in Octave in the domain $\left[\zeta_{\mathcal{P}}, \zeta_{\mathcal{X}}\right]$ created via the definition of ζ from the two-dimensional domain $\left[r_{\mathcal{P}}, r_{\mathcal{X}}\right] \times \left[t_{\text{fail}}/40, 10t_{\text{fail}}\right]$, where the partial differential equation was solved. This interval was chosen so as to avoid undue proximity to $t = 0$, where the solution coincides with the steady state – a lesson learnt from the slow variation regime, and to cover the extent where the non-linearity effect was fully visible before the new steady state was attained. At each iteration an integration was performed over the segment $\left[\zeta_{\mathcal{P}}, \zeta_{\mathcal{A}}\right]$ with the initial condition

$$y_1\left(\zeta_{\mathcal{P}}\right) = p\left(r_{\mathcal{P}}, \tau\right) \tag{20b}$$

conforming to (4a) and $y_2\left(\zeta_{\mathcal{P}}\right)$ given an initial guess, followed by a second integration over the segment $\left[\zeta_{\mathcal{A}}, \zeta_{\mathcal{X}}\right]$ with the initial conditions

$$y_1\left(\zeta_{\mathcal{A}}^+\right) = y_1\left(\zeta_{\mathcal{A}}^-\right), \qquad y_2\left(\zeta_{\mathcal{A}}^+\right) = \frac{k_a}{k_x}\, y_2\left(\zeta_{\mathcal{A}}^-\right) \tag{20c}$$

that convert (3) to the ζ domain for any fixed value of t. The ensuing value $y_1\left(\zeta_{\mathcal{X}}\right)$ was used to modify $y_2\left(\zeta_{\mathcal{P}}\right)$ until convergence, i.e. $y_1\left(\zeta_{\mathcal{X}}\right) = p\left(r_{\mathcal{X}}, \tau\right)$ up to a predefined tolerance of 10^{-6}. Octave built-in function `fsolve` was used to implement the iterative procedure.

Figure 9 compares the resulting pressure profiles to a full numerical solution. The deviation exemplified for moderate permeability disparity between the two laminae deteriorates further for higher ratios k_a/k_x. Therefore the reduction of the partial differential equation (2b) to the affinity equation (19) is not valid in that part of the parameter space.

5 Conclusion

The weakly compressible flow through a porous medium is governed by a unique partial differential equation solvable as linear in p^2 when the flow is steady, but becoming non-linear when a temporal dependence is involved. Applications such as landfill gas, natural gas or sparging wells might have their steady operation disrupted by a pump failure or influenced by recurring fluctuations of the atmospheric pressure and water table. The response might be a one way transition to a new equilibrium or an ongoing evolution, where the steady state is never approached. Both types of response might be quasi-equilibrial or fast varying.

In the quasi-steady regime the pressure distribution throughout the domain has sufficient time to adjust to the temporal variation at a boundary, endowing the system with an asymptotic solution. Whilst any time dependent system will possess such a regime, the non-trivial question is how extensive a parameter space supports it. Juxtaposition of the results of a full numerical simulation and the asymptotics revealed that in this problem the relevant parameter space encompasses all feasible values of both the intrinsic porous matrix properties and the well's functional specifications controlled by the operators. The associated error is well beneath the desirable threshold set by the resolution of commonly available instrumentation for a wide range of imposed suction strength values as well as four orders of magnitude in lamina permeability disparity. Furthermore, the formally small parameter ϵ in practice can approach unity before the accuracy of the asymptotic solution with only a single correction term deteriorates. The variation induced on the boundary might be any non-linear generic function of time and prescribe either pressure (Dirichlet condition) or flux (Neumann condition). Such a wide domain of validity is rare in practical problems, rendering the value of the asymptotic solution very high: without advanced algorithms solving partial differential equations well designers and field operators can predict the pressure distribution in the porous matrix in response to various disruptions or fluctuations in the conditions reigning in the surroundings of the well facility.

In light of the above, although formally this regime must be referred to as slow or quasi-steady, in reality $\epsilon \sim \mathcal{O}(1)$ implies a reaction time of 1 second and should be thought of as adequately spanning the slow to fast realistic time scale. By comparison, the fast regime is extremely fast: the boundary condition must attain order of unity change within 0.01 seconds or less, and the response lasts only 0.1 seconds before the new equilibrium is approached.

The fast response might be obtained by reduction of the partial differential equation to an ordinary equation via an affinity variable. The ensuing accuracy is adequate for practical usage over a limited part of the parameter space. Although the affinity reduction itself has been known for many decades in the context of the partial differential equation in question, the domain, boundary conditions and discontinuous intrinsic matrix properties of the current problem required a completely new iterative approach. The solution is valid for low and moderate permeability ratios $1 \lessapprox k_a/k_x \lessapprox 100$. For higher ratios no simplification of the partial differential equation is forthcoming.

The asymptotic and affinity solutions are valuable well design and control tools, enabling investigation of the flow field for a variety of time dependent boundary conditions with the view to determine compliance with regulations specifying permissible pressure threshold, extracted gas quantity and boundary flux. The ability to access time dependent pressure profiles within the landfill mass is essential to estimate the resultant zone of influence and when optimising the energy required to operate the collection system.

Acknowledgement

The authors are grateful to Prof. A.A. Nepomnyashchy for helpful discussions on the evolution of similarity and affinity concepts.

References

Barenblatt GI (1996) Scaling, self-similarity and intermediate asymptotics. Cambridge University Press
Barenblatt GI, Entov VM, Ryzhik VM (1990) Theory of fluid flow through natural rock. Kluwer, Dodrecht
Conestoga-Rovers A (2010) Landfill gas management facilities design guidelines. Tech. rep., British Columbia Ministry of Environment
Davidson TA (1993) A simple and accurate method for calculating viscosity of gaseous mixtures. Report of investigations, US Department of the Interior, Bureau of Mines.
Feng SJ, Zheng QT, Xie HJ (2015) A model for gas pressure in layered landfills with horizontal gas collection systems. Comput Geotech 68:117–127
Feng SJ, Zheng QT, Xie HJ (2017) A gas flow model for layered landfills with vertical extraction wells. Waste Management 66:101–113
Fulks WB, Guenther RB, Roetman EL (1971) Equations of motion and continuity for fluid flow in a porous medium. Acta Mechanica 12:121–129
GNU Octave (2021) 6.2.0. *https://www.gnu.org/software/octave/index*
Halvorsen D, Nec Y, Huculak G (2018) Horizontal landfill gas wells: geometry, physics of flow and connection with the atmosphere. Phys Chem Earth 113:50–62
Hyman JD, Karra S, Makedonska N, Gable CW, Painter SL, Viswanathan HS (2015) dfnworks: a discrete fracture network framework for modeling subsurface flow and transport. Comp Geosci 84:10–19
Keenan S, Nec Y, Huculak G (2021) Landfill gas flow: effects of asymmetry. J Solid Waste Tech Management 47(1):188–203
King JR (1988) Approximate solutions to a nonlinear diffusion equation. J Eng Math 22:53–72
Kutsyi DV (2015) Numerical modeling of landfill gas and heat transport in the deformable MSW landfill body. Part 2. Verification and application of the model. Thermal Engineering 62(7):495–502
Lakhtakia A, Messier R, Varadan VV, Varadan VK (1986) Self-similarity versus self-affinity: the sierpinski gasket revisited. J Phys A: Math Gen 19:L985
Lundegard PD, LaBrecque D (1995) Air sparging in a sandy aquifer (Florence,Oregon, U.S.A.): actual and apparent radius of influence. J Contaminant Hydrology 19:1–27
Mandelbrot BB (1985) Self-affine fractals and fractal dimension. Phys Scr 32:257
Nec Y, Huculak G (2019) Landfill gas flow: collection by horizontal wells. Transport in Porous Media 130(3):769–797
PDE Solutions Inc. (2016) Flexpde 7. *http://www.pdesolutions.com*
Volpert VA, Nepomnyashchy AA, Kanevsky Y (2018) Drug diffusion in a swollen polymer. SIAM J Appl Math 78(1):124–144
Whitaker S (1986) Flow in porous media I: a theoretical derivation of Darcy's law. Transport in Porous Media 1:3–25
Wise WR, Townsend TG (2011) One-dimensional gas flow models for municipal solid waste landfills: cylindrical and spherical symmetries. J Environ Eng 137(6):514–516
Young A (1989) Mathematical modeling of landfill gas extraction. J Environ Eng 115(6):1073–1087

Declarations

Funding The support of Canada Foundation for Innovation grant # 35174 as well as Thompson Rivers University Undergraduate Research Apprenticeship programme is gratefully acknowledged.

Conflict of interest The authors declare no conflict of interest.

Availability of data and material Not applicable.

Code availability Not applicable.

Appendix A. Slow variation regime: permeable outermost boundary

Replacing (5b) by a Dirichlet condition with a pressure function $p_{\mathcal{X}}(\tau) \sim \mathcal{O}(1)$ on the outermost circumference, (9b) becomes

$$p_0(r_{\mathcal{X}},\tau) = p_{\mathcal{X}}(\tau), \qquad p_i(r_{\mathcal{X}},\tau) = 0 \quad \forall\ i \geqslant 1. \tag{A1a}$$

Combining this with (9a) and (10a), the leading order solutions are given by (11) with

$$\begin{aligned}
A_0^{(a)}(\tau) &= \left\{ p_{\mathcal{X}}^2(\tau) - p_{\text{well}}^2(\tau) + \frac{\mu C_b}{k_x}\left(\frac{1}{2}\left(r_{\mathcal{X}}^2 - r_{\mathcal{A}}^2\right) + r_{\mathcal{A}}^2 \ln\frac{r_{\mathcal{A}}}{r_{\mathcal{X}}}\right)\right\} \Bigg/ \left\{ \ln\frac{r_{\mathcal{A}}}{r_{\mathcal{P}}} - \frac{k_a}{k_x}\ln\frac{r_{\mathcal{A}}}{r_{\mathcal{B}}}\right\},\\
A_0^{(b)}(\tau) &= \frac{k_a}{k_x}\, A_0^{(a)} + \frac{\mu C_b}{k_x}\, r_{\mathcal{A}}^2,\\
B_0^{(a)}(\tau) &= p_{\text{well}}^2(\tau) - A_0^{(a)}(\tau)\ln r_{\mathcal{P}},\\
B_0^{(b)}(\tau) &= p_{\mathcal{X}}^2(\tau) - A_0^{(b)}(\tau)\ln r_{\mathcal{X}} + \frac{\mu C_b}{2k_x}\, r_{\mathcal{X}}^2.
\end{aligned} \tag{A1b}$$

These coefficients are identical to those obtained for the steady state bar the notation for the boundary conditions that herein are time dependent functions, cf. equation (B1) in Appendix B of Nec and Huculak (2019). Note that even if $p_{\mathcal{X}}$ is taken constant, all four coefficients will nonetheless be τ-dependent, thereby precluding the uncoupling attained with a sealed boundary (15). The underpinning physical reason is the finite permeability of the boundary $r = r_{\mathcal{X}}$, be it due to a pressure condition or a prescribed flux function, as is seen hereunder. The correction is given by

$$\begin{aligned}
\left(p_0 p_1\right)^{(a)} &= \frac{\mu\varphi_a}{2k_a}\int_{r_{\mathcal{P}}}^{r}\frac{1}{\tilde{r}}\int_{r_{\mathcal{A}}}^{\tilde{r}}\frac{\varrho}{p_0^{(a)}(\varrho,\tau)}\left(\frac{\mathrm{d}A_0^{(a)}}{d\tau}\ln\rho + \frac{\mathrm{d}B_0^{(a)}}{d\tau}\right)\mathrm{d}\varrho\,\mathrm{d}\tilde{r} + A_1^{(a)}(\tau)\ln r + B_1^{(a)}(\tau),\\
\left(p_0 p_1\right)^{(b)} &= \frac{\mu\varphi_x}{2k_x}\int_{r_{\mathcal{X}}}^{r}\frac{1}{\tilde{r}}\int_{r_{\mathcal{A}}}^{\tilde{r}}\frac{\varrho}{p_0^{(b)}(\varrho,\tau)}\left(\frac{\mathrm{d}A_0^{(b)}}{d\tau}\ln\rho + \frac{\mathrm{d}B_0^{(b)}}{d\tau}\right)\mathrm{d}\varrho\,\mathrm{d}\tilde{r} + A_1^{(b)}(\tau)\ln r + B_1^{(b)}(\tau)
\end{aligned} \tag{A1c}$$

with the coefficients satisfying the following linear system:

$$\begin{pmatrix} k_a & 0 & -k_x & 0\\ \ln r_{\mathcal{P}} & 1 & 0 & 0\\ 0 & 0 & \ln r_{\mathcal{X}} & 1\\ \ln r_{\mathcal{A}} & 1 & -\ln r_{\mathcal{A}} & -1 \end{pmatrix}\begin{pmatrix} A_1^{(a)}\\ B_1^{(a)}\\ A_1^{(b)}\\ B_1^{(b)}\end{pmatrix} = \begin{pmatrix} 0\\ 0\\ 0\\ I\end{pmatrix}, \tag{A1d}$$

where

$$I = \frac{\mu\varphi_x}{2k_x}\int_{r_{\mathcal{X}}}^{r_{\mathcal{A}}}\frac{1}{\tilde{r}}\int_{r_{\mathcal{A}}}^{\tilde{r}}\frac{\varrho}{p_0^{(b)}(\varrho,\tau)}\left(\frac{\mathrm{d}A_0^{(b)}}{d\tau}\ln\rho + \frac{\mathrm{d}B_0^{(b)}}{d\tau}\right)\mathrm{d}\varrho\,\mathrm{d}\tilde{r} - \frac{\mu\varphi_a}{2k_a}\int_{r_{\mathcal{P}}}^{r_{\mathcal{A}}}\frac{1}{\tilde{r}}\int_{r_{\mathcal{A}}}^{\tilde{r}}\frac{\varrho}{p_0^{(a)}(\varrho,\tau)}\left(\frac{\mathrm{d}A_0^{(a)}}{d\tau}\ln\rho + \frac{\mathrm{d}B_0^{(a)}}{d\tau}\right)\mathrm{d}\varrho\,\mathrm{d}\tilde{r}. \tag{A1e}$$

When wishing to prescribe a non-zero velocity value on the outermost boundary $u_{\mathcal{X}}(\tau) = -\dfrac{k_x}{\mu}\dfrac{\partial p}{\partial r}\Big|_{(r_{\mathcal{X}},\tau)}$ instead of (5b), (9b) becomes

$$-\frac{k_x}{\mu}\frac{\partial p_0}{\partial r}\bigg|_{(r_{\mathcal{X}},\tau)} = u_{\mathcal{X}}(\tau), \quad \frac{\partial p_i}{\partial r}\bigg|_{(r_{\mathcal{X}},\tau)} = 0\ \forall\ i \geqslant 1. \tag{A2a}$$

Applying the first condition above and (9a) to (11b) and (11a) respectively, in conjunction with (10a) yields

$$\left(\frac{A_0^{(b)}}{r_{\mathcal{X}}} - \frac{\mu C_b}{k_x}\, r_{\mathcal{X}}\right)^2 = 4\left(\frac{\mu u_{\mathcal{X}}(\tau)}{k_x}\right)^2\left\{A_0^{(b)}\left(\ln\frac{r_{\mathcal{X}}}{r_{\mathcal{A}}} + \frac{k_x}{k_a}\ln\frac{r_{\mathcal{A}}}{r_{\mathcal{P}}}\right) + p_{\text{well}}^2(\tau) + \frac{\mu C_b}{k_x}\left(\frac{1}{2}\left(r_{\mathcal{A}}^2 - r_{\mathcal{X}}^2\right) - \frac{k_x}{k_a}\, r_{\mathcal{A}}^2\ln\frac{r_{\mathcal{A}}}{r_{\mathcal{P}}}\right)\right\}. \tag{A2b}$$

This is a quadratics in $A_0^{(b)}(\tau)$, whose two solutions correspond to $\left|u_{\mathcal{X}}(\tau)\right|$, with one to be chosen based on the desired sign of $u_{\mathcal{X}}(\tau)$. With that

$$A_0^{(a)}(\tau) = \frac{k_x}{k_a}\, A_0^{(b)}(\tau) - \frac{\mu C_b}{k_a}\, r_{\mathcal{A}}^2, \tag{A2c}$$

$$B_0^{(a)}(\tau) = p_{\text{well}}^2(\tau) - A_0^{(a)}(\tau)\ln r_{\mathcal{P}}, \tag{A2d}$$

allowing to construct (11a). Then

$$B_0^{(b)}(\tau) = {p_0^{(a)}}^2\big(r_{\mathcal{A}},\tau\big) - A_0^{(b)}(\tau)\ln r_{\mathcal{A}} + \frac{\mu C_b}{2k_x}\, r_{\mathcal{A}}^2. \tag{A2e}$$

The correction equations will follow (13) and (14):

$$\begin{aligned}
\big(p_0 p_1\big)^{(a)} &= \frac{\mu\varphi_a}{2k_a}\int_{r_{\mathcal{P}}}^{r}\frac{1}{\tilde r}\int_{r_{\mathcal{A}}}^{\tilde r}\frac{\varrho}{p_0^{(a)}(\varrho,\tau)}\left(\frac{\mathrm{d}A_0^{(a)}}{d\tau}\,\ln\rho + \frac{\mathrm{d}B_0^{(a)}}{d\tau}\right)\mathrm{d}\varrho\,\mathrm{d}\tilde r + A_1^{(a)}(\tau)\ln r + B_1^{(a)}(\tau),\\
\big(p_0 p_1\big)^{(b)} &= \frac{\mu\varphi_x}{2k_x}\int_{r_{\mathcal{A}}}^{r}\frac{1}{\tilde r}\int_{r_{\mathcal{X}}}^{\tilde r}\frac{\varrho}{p_0^{(b)}(\varrho,\tau)}\left(\frac{\mathrm{d}A_0^{(b)}}{d\tau}\,\ln\rho + \frac{\mathrm{d}B_0^{(b)}}{d\tau}\right)\mathrm{d}\varrho\,\mathrm{d}\tilde r + A_1^{(b)}(\tau)\ln r + B_1^{(b)}(\tau)
\end{aligned} \tag{A2f}$$

with

$$\begin{aligned}
A_1^{(b)} &= 0,\\
A_1^{(a)} &= \frac{\mu\varphi_x}{2k_a}\int_{r_{\mathcal{X}}}^{r_{\mathcal{A}}}\frac{\varrho}{p_0^{(b)}(\varrho,\tau)}\left(\frac{\mathrm{d}A_0^{(b)}}{d\tau}\,\ln\rho + \frac{\mathrm{d}B_0^{(b)}}{d\tau}\right)\mathrm{d}\varrho,\\
B_1^{(a)} &= -A_1^{(a)}\ln r_{\mathcal{P}},\\
B_1^{(b)} &= \frac{\mu\varphi_a}{2k_a}\int_{r_{\mathcal{P}}}^{r_{\mathcal{A}}}\frac{1}{\tilde r}\int_{r_{\mathcal{A}}}^{\tilde r}\frac{\varrho}{p_0^{(a)}(\varrho,\tau)}\left(\frac{\mathrm{d}A_0^{(a)}}{d\tau}\,\ln\rho + \frac{\mathrm{d}B_0^{(a)}}{d\tau}\right)\mathrm{d}\varrho\,\mathrm{d}\tilde r + A_1^{(a)}\ln\frac{r_{\mathcal{A}}}{r_{\mathcal{P}}}\,.
\end{aligned} \tag{A2g}$$

In (A2f) the time derivatives of $A_0^{(a)}(\tau)$, $B_0^{(a)}(\tau)$ and $B_0^{(b)}(\tau)$ are obtained directly from (A2c)–(A2e). The time derivative of $A_0^{(b)}(\tau)$ follows by the differentiation of (A2b).